REST/NRSF governs the expression of dense-core vesicle gliosecretion in astrocytes

Ilaria Prada,[1,2] Julie Marchaland,[3] Paola Podini,[1,2] Lorenzo Magrassi,[4] Rosalba D'Alessandro,[1,2] Paola Bezzi,[3] and Jacopo Meldolesi[1,2]

[1]San Raffaele Scientific Institute, 20132 Milan, Italy
[2]Research Unit of Molecular Neuroscience, Italian Institute of Technology Network, 20132 Milan, Italy
[3]Department of Cell Biology and Morphology, University of Lausanne, 1005 Lausanne, Switzerland
[4]Neurosurgery, Department of Surgical Sciences, University of Pavia, Policlinico San Matteo Foundation, 27100 Pavia, Italy

Astrocytes are the brain nonnerve cells that are competent for gliosecretion, i.e., for expression and regulated exocytosis of clear and dense-core vesicles (DCVs). We investigated whether expression of astrocyte DCVs is governed by RE-1–silencing transcription factor (REST)/neuron-restrictive silencer factor (NRSF), the transcription repressor that orchestrates nerve cell differentiation. Rat astrocyte cultures exhibited high levels of REST and expressed neither DCVs nor their markers (granins, peptides, and membrane proteins). Transfection of a dominant-negative construct of REST induced the appearance of DCVs filled with secretogranin 2 and neuropeptide Y (NPY) and distinct from other organelles. Total internal reflection fluorescence analysis revealed NPY–monomeric red fluorescent protein–labeled DCVs to undergo Ca^{2+}-dependent exocytosis, which was largely prevented by botulinum toxin B. In the I–II layers of the human temporal brain cortex, all neurons and microglia exhibited the expected inappreciable and high levels of REST, respectively. In contrast, astrocyte REST was variable, going from inappreciable to high, and accompanied by a variable expression of DCVs. In conclusion, astrocyte DCV expression and gliosecretion are governed by REST. The variable in situ REST levels may contribute to the well-known structural/functional heterogeneity of astrocytes.

Introduction

Expression of neurotransmitter-containing vesicles, i.e., small clear vesicles (CVs) and dense-core vesicles (DCVs), and their Ca^{2+}-induced exocytosis were considered, for long time, to be specific properties of neurons and neurosecretory cells (indicated together as nerve cells). However, substantial evidence accumulated during the last 15 yr demonstrates that a form of exocytic neurotransmitter release, commonly called gliotransmission (Bezzi and Volterra, 2001; Zhang and Haydon, 2005; Theodosis et al., 2008), also takes place from a specific type of nonnerve cell, the astrocytes of the brain (Volterra and Meldolesi, 2005; Haydon and Carmignoto, 2006; Hamilton and Attwell, 2010; Parpura and Zorec, 2010), especially at the level of the processes enwrapping the pre- and postsynaptic compartments of synapses (tripartite synapses; Araque et al., 1999; Jourdain et al., 2007; Perea et al., 2009). Consistently, astrocytes were found to have a role in complex functions of the nervous system, such as synaptogenesis, plasticity of synapses, and circuits, and also behavior (Araque and Navarrete, 2010; Halassa and Haydon, 2010; Paixão and Klein, 2010). Formerly considered simple scaffold cells, astrocytes are therefore recognized as having a much higher rank in the functioning of the brain.

In cell biological terms, knowledge of gliotransmission is much less detailed than that of neurotransmission. In particular, most of the available information refers primarily to CVs. Extensive evidence indicates, in fact, that low molecular weight

Correspondence to Jacopo Meldolesi: meldolesi.jacopo@hsr.it; or Paola Bezzi: paola.bezzi@unil.ch

R. D'Alessandro's present address is Saverio de Bellis Scientific Institute, 70013 Castellana Grotte Bari, Italy.

Abbreviations used in this paper: BoNT/B, botulinum toxin B; ChgA, chromogranin A; ChgB, chromogranin B; CV, clear vesicle; DBD, DNA-binding domain; DCV, dense-core vesicle; EPI, epillumination; GFAP, glial fibrillary acidic protein; GS, glutamine synthase; mRFP, monomeric RFP; NeuN, neuronal nuclei; NPY, neuropeptide Y; RIPA, radioimmunoprecipitation assay; RE-1, restrictive element-1; REST, RE-1–silencing transcription factor; RT-PCR, real-time PCR; Sg2, secretogranin 2; shRNA, small hairpin RNA; Stx1a, syntaxin 1a; TfR, transferrin receptor; TIRF, total internal reflection fluorescence; wtPC12, wild-type PC12.

The Rockefeller University Press $30.00
J. Cell Biol. Vol. 193 No. 3 537–549
www.jcb.org/cgi/doi/10.1083/jcb.201010126

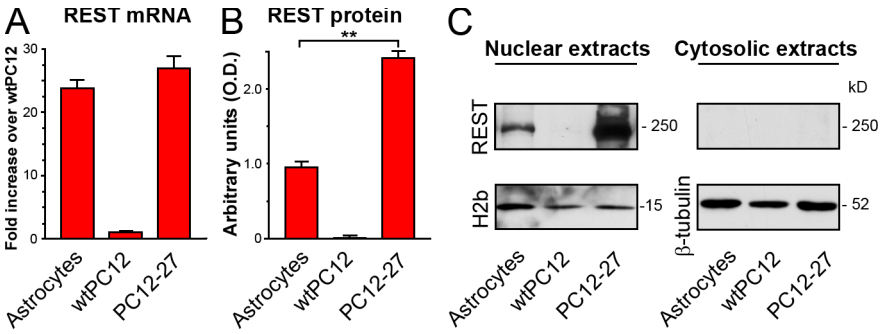

Figure 1. **Expression and intracellular distribution of REST in cultured astrocytes and PC12 cell clones.** (A) The levels of REST mRNA in cultured astrocytes that are much higher than those of wtPC12 and similar to those of the high REST PC12 clone PC12-27. Error bars indicate SEM. (B and C) Western blot results concerning the 225-kD band (C) decorated by the Millipore anti-REST pAb. Proteomic analyses (to be reported elsewhere) demonstrated the 225-kD band to contain only REST; other major bands, also decorated by the pAb (not depicted), were shown to contain unrelated proteins. The astrocyte REST protein levels, ∼40% of those of PC12-27 cells, are shown in B (**, $P < 0.01$; error bars show SD). C shows the REST Western blots of the nuclear and cytoplasmic extracts of the three cell types, revealing the concentration of the REST protein in the nucleus (left) with inappreciable levels in the cytoplasm (right). Data are from three experiments performed in triplicate.

transmitters, such as glutamate and D-serine (Bezzi et al., 2004; Mothet et al., 2005; Panatier et al., 2006; Jourdain et al., 2007; Marchaland et al., 2008; Martineau et al., 2008; Bergersen and Gundersen, 2009), accumulate within these vesicles both in cultured astrocytes and in the perisynaptic processes of the hippocampus. At the ultrastructural level, CVs have been identified (30–80-nm-diameter, round, clear lumen) in the proximity or in direct contact with the plasma membrane (Jourdain et al., 2007; Bergersen and Gundersen, 2009).

CVs, however, are not the only gliosecretory vesicles. Cultured astrocytes investigated by various groups were found to contain DCVs that were also recently reported in the human brain tissue (Hur et al., 2010). Astrocyte DCVs exhibit the typical ultrastructure, which is analogous to the DCVs of nerve cells. Moreover, their cargo molecules, i.e., the proteins secretogranin 2 (Sg2; Calegari et al., 1999; Paco et al., 2009) and secretogranin 3 (Paco et al., 2010), the atrial natriuretic peptide (Kreft et al., 2004), and neuropeptide Y (NPY; Ramamoorthy and Whim, 2008), and also ATP (Coco et al., 2003; Pangrsic et al., 2007) are discharged upon stimulation. The identification of the astrocyte DCVs was validated by the characterization of their exocytosis (Pangrsic et al., 2007; Ramamoorthy and Whim, 2008). Yet, in various laboratories, expression of DCVs in astrocyte cultures was never demonstrated beyond doubt.

The present study, which was performed in cultures of rat astrocytes and in astrocytes of the human brain cortex, investigates the possibility that astrocyte expression of DCVs depends on RE-1–silencing transcription factor (REST; otherwise called NRSF [neuron-restrictive silencer factor]), the transcription repressor encoded by the master gene that orchestrates differentiation of nerve cells (Ballas and Mandel, 2005; Ooi and Wood, 2007). A rapid and large decrease of REST, occurring at a late nerve cell precursor stage, is known to derepress the transcription of hundreds of genes, many of which are specific, and to induce the acquisition of multiple aspects of the nerve cell phenotype, including DCVs and their exocytosis (Bruce et al., 2006; D'Alessandro et al., 2008). In contrast, the persistence of REST at high levels, which is typical of differentiated nonnerve cells (Ballas and Mandel, 2005; Ooi and Wood, 2007), is believed to preclude the expression of many nerve cell–specific features, including DCVs (Bruce et al., 2006; D'Alessandro et al., 2008). Whether REST levels in astrocytes are as high as in the other nonnerve cells is unclear. In a pioneer study of the rat adult brain, REST mRNA was reported to be as low in astrocytes as in neurons (Palm et al., 1998), whereas recently, the REST protein was found to be high in rat astrocytes in culture (Kohyama et al., 2010). The consequences of these high levels in terms of DCV expression were not investigated.

Our evidence, which was obtained by various approaches, now demonstrates that in rat astrocyte cultures, the expression of DCVs and of their regulated discharge is indeed governed by REST. In the standard conditions of our cultures, REST was high, and the DCVs together with their markers were almost completely lacking. When, however, repression was attenuated by transfection of a dominant-negative construct of REST, DCVs appeared and were discharged upon stimulation by an exocytic process that was sensitive to botulinum toxin B (BoNT/B). In addition, immunocytochemistry of the human brain cortex revealed that in situ, the single astrocyte levels of REST are variable, from as low as in neurons to as high as in microglia. Such heterogeneity, which has never been reported in any type of cell, could explain at least part of the conflicting results previously obtained by different laboratories in terms of DCVs and their gliotransmission. In addition, the variable levels of REST could play a role in the structural and functional heterogeneity of the various forms of astrocytes, a long-known property that is still largely unexplained (Volterra and Meldolesi, 2005; Oberheim et al., 2006; Wang and Bordey, 2008; Hewett, 2009; Matyash and Kettenmann, 2010).

Results

REST and neuro/gliosecretion proteins in cultured astrocytes

In view of the conflicting data in the literature (Palm et al., 1998; Kohyama et al., 2010), our first purpose was to establish the levels and the nuclear/cytoplasmic distribution of REST in astrocyte primary cultures grown as described previously (Bezzi et al., 2001; Marchaland et al., 2008). As reference models, we used two clones of the rat pheochromocytoma PC12 cell line

expressing different levels of REST, i.e., a wild-type clone characterized by the low levels typical of nerve cells and a clone defective of neurosecretion because of its high levels of the transcription repressor (PC12-27; D'Alessandro et al., 2008). Fig. 1 A shows that in astrocytes, the REST mRNA (assayed by real-time PCR [RT-PCR]) was only slightly lower and much higher than those of the PC12-27 and wild-type PC12 (wtPC12) clones, respectively. The corresponding REST protein, although only ~40% of the high REST PC12-27 cells, was still a tenth of a fold higher than the wtPC12 (Fig. 1 B). In spite of these differences, the intracellular distribution of REST in astrocytes and in the two PC12 clones investigated by subcellular fractionation was the same, i.e., almost completely nuclear (Fig. 1 C).

We then investigated the levels of various proteins possibly involved in gliosecretion. Previous studies of these proteins in astrocyte cultures had yielded partially conflicting results (summarized in Volterra and Meldolesi, 2005). Fig. 2 shows that our cultured astrocytes resembled the high REST PC12-27 clone in their low expression or absence of many proteins typical of nerve cell DCVs and of their exocytic discharge: the three cargo granins chromogranin A (ChgA), chromogranin B (ChgB), and Sg2 (Fig. 2 A), two vesicle membrane proteins Syt1 (synaptotagmin 1) and Syp1 (synaptophysin 1), the t-SNARE SNAP25, and the small GTPase Rab3a. Syt4 and Munc18 were also low in cultured astrocytes as in high REST PC12-27. However, they were closer to the wtPC12 levels. Only the t-SNARE syntaxin 1a (Stx1a), although lower than in the wtPC12, was distinctly higher in astrocytes than in the high REST PC12-27. Finally, VAMP2, the v-SNARE of nerve cell CVs and DCVs, and VAMP3 and SNAP23, two SNAREs not involved in neurosecretion but possibly involved in gliosecretion and other membrane fusion processes, were expressed at similar or even higher levels in astrocytes and high REST PC12-27 than in wtPC12 cells (Fig. 2, B and C). The direct role of REST in the repression of at least one of the proteins investigated in astrocytes, the t-SNARE SNAP25, was confirmed by chromatin immunoprecipitation (Fig. S1).

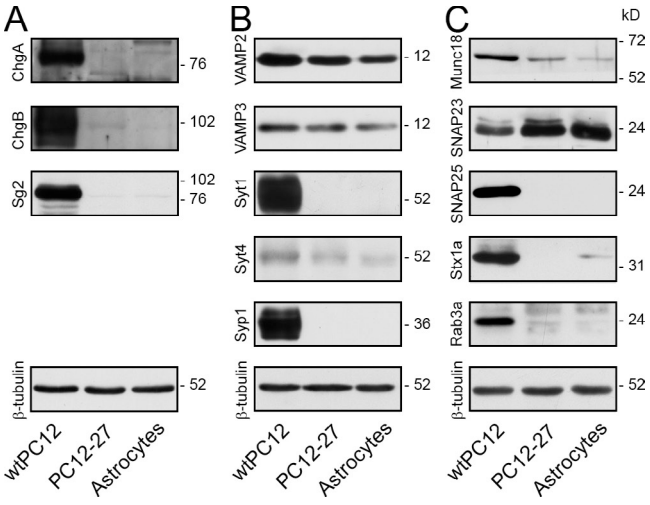

Figure 2. **Expression of neuro/gliosecretion proteins in cultured astrocytes, in wtPC12, and in high REST PC12-27 cells.** (A–C) The figure, representative of the results obtained from at least three experiments, illustrates the levels of various proteins: cargo proteins (A); vesicle membrane proteins (B); and soluble and t-SNARE proteins (C). Various proteins present and even abundant in wtPC12 cells (such as the cargo proteins ChgA, ChgB, and Sg2 [A], the vesicle membrane proteins Syt1 and Syp1, Rab3a, and the t-SNARE SNAP25 [B and C]) are absent or hardly appreciable in astrocytes and PC12-27 cells. Stx1a and Munc18 (C) are low but appreciable. The only proteins well represented in astrocytes and high REST PC12-27 are VAMP2, Syt4, VAMP3, and SNAP23 (B and C). The last two, which are not directly involved in neurosecretion, may have a role in gliosecretion (Volterra and Meldolesi, 2005).

Transfection of a dominant-negative construct of REST induces the expression of some gliosecretion genes and appearance of DCVs

Cultured rat astrocytes were transiently transfected with REST/DNA-binding domain (DBD)–GFP, a dominant-negative construct that includes the DBD of REST coupled to GFP (D'Alessandro et al., 2008). Previous results with PC12 demonstrated this construct to compete with the repressor for binding to the restrictive element-1 (RE-1) sequence of gene promoters. The construct therefore attenuates the specific tone of REST repression (Bruce et al., 2006; Pance et al., 2006; D'Alessandro et al., 2008; Klajn et al., 2009). Control astrocytes of these experiments were transfected with the same plasmid that included, however, GFP only. Fluorescent cells transfected with either GFP alone or REST/DBD-GFP were then sorted out by FACS before analysis. Fig. 3 (A–C) shows that among the genes encoding proteins typical of nerve cell DCVs or involved in their exocytic discharge, the REST/DBD-GFP construct increased the expression of only three of them, SNAP25, Stx1a, and Sg2. In particular, the SNAP25 mRNA and protein became appreciable, and those of Stx1a increased slightly, whereas those of Sg2 increased almost threefold and over sevenfold (Fig. 3, A and C). Compared with wtPC12, the Sg2 protein reached a level of ~8% (Fig. 3 C). In contrast, the levels of three astrocyte markers, glutamine synthase (GS), glial fibrillary acidic protein (GFAP), and S100β, remained unchanged (Fig. 3, D and E), confirming the bona fide astrocyte nature of the transfected cells.

The effect of REST/DBD-GFP on Sg2 protein expression was also clearly visible by immunocytochemistry. In all control astrocytes transfected with GFP alone, no Sg2 signal was appreciable (Fig. 4 A). In contrast, >95% of the astrocytes transfected with the REST/DBD-GFP construct exhibited numerous puncta that were clearly positive for Sg2, scattered in the cytoplasm, and aligned near the plasma membrane (Fig. 4 B). Of these puncta, ~80% were positive also for endogenous NPY (Fig. 4 C). In contrast, when the REST/DBD-GFP–transfected astrocytes were dually immunolabeled for Sg2 together with markers of intracellular organelles (TGN38 of the TGN, Lamp1 of lysosomes, EEA1 of early endosomes, or transferrin receptor [TfR] of late endosomes), no colocalization above the background level (<5%) was observed in the Sg2-positive puncta (Fig. 4, F–I).

When the REST/DBD-GFP–transfected astrocytes were studied by electron microscopy, they exhibited typical DCVs (Fig. 4, D and D') with an mean diameter (corrected as in Parsons et al., 1995) of 170 ± 40 nm (n = 32), which were distributed both in the depth of the cytoplasm and in the layer adjacent to the plasma membrane. These DCVs were intensely immunogold labeled for the Sg2 segregated within their lumen. In a few cases, they

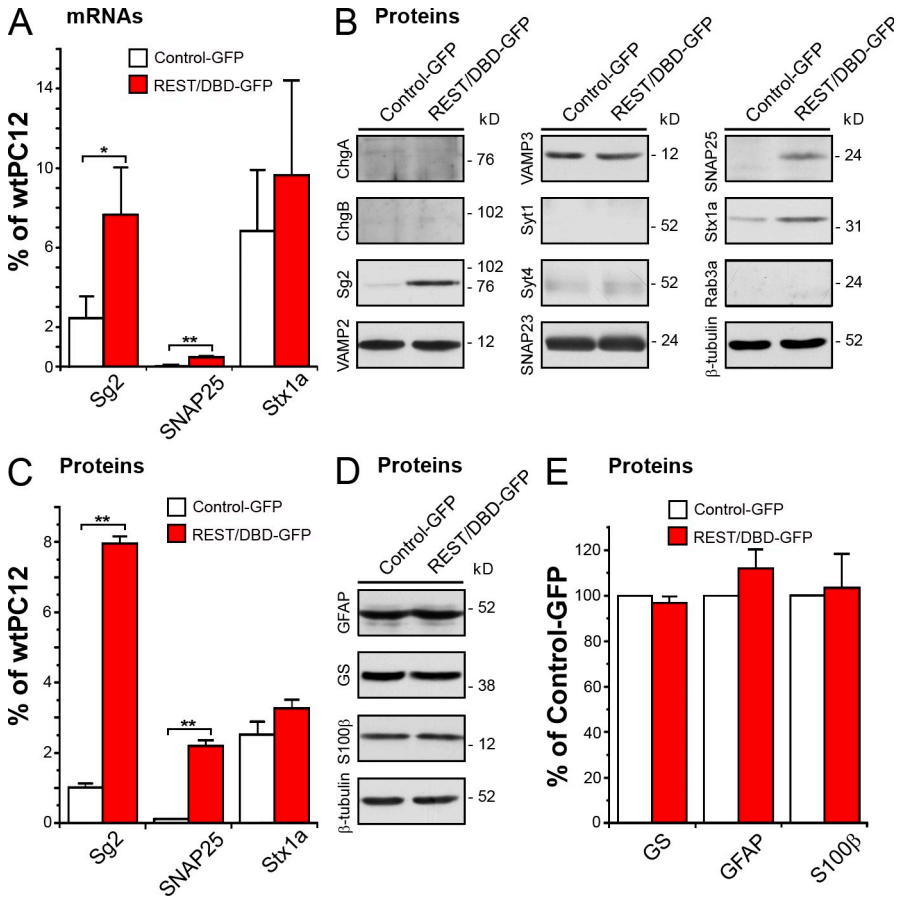

Figure 3. **Expression of neuro/gliosecretion proteins in cultured astrocytes transfected with GFP or with the dominant-negative construct REST/DBD-GFP.** (B) Representative Western blots illustrating the expression of eleven neuro/gliosecretion proteins in the two transfected astrocyte populations. (A and C) Notice that in eight of them, the levels are unaffected by the dominant-negative construct, whereas in three, Sg2, SNAP25, and Stx1a, gene expression is increased at both the mRNA (A) and the protein (C) level. Error bars indicate SEM (A) and SD (C). *, $P < 0.05$; **, $P < 0.01$. (D and E) Transfection of REST/DBD-GFP does not change the expression of three astrocyte protein markers, GS, GFAP, and S100β. Results are from three experiments performed in triplicate. Error bars indicate SD.

were seen during discharge to the extracellular space (Fig. 4 E). We conclude that the attenuation of the endogenous REST tone by the transfected REST/DBD-GFP construct induces, in our cultured astrocytes, the appearance of bona fide DCVs, which were positive for the specific markers and analogous to those previously reported by others in cultured astrocytes independently of the REST/DBD-GFP transfection (Calegari et al., 1999; Kreft et al., 2004; Ramamoorthy and Whim, 2008; Paco et al., 2010).

Astrocytes cotransfected with REST/DBD-GFP and NPY-monomeric RFP (mRFP) accumulate DCVs positive for both the endogenous Sg2 and the exogenous fluorescent peptide

In the data illustrated so far, we reported the appearance of DCVs and their endogenous components (Sg2 and NPY) taking place in cultured astrocytes upon transfection of the REST dominant-negative construct REST/DBD-GFP. To establish whether these DCVs were discharged by regulated exocytosis, we used total internal reflection fluorescence (TIRF) by which the dynamics and discharge of fluorescent puncta (in our case DCVs loaded with NPY-mRFP; Ramamoorthy and Whim, 2008) is investigated in the 92-nm-thick superficial layer of the cytoplasm illuminated by the evanescent wave (Marchaland et al., 2008). Before carrying out the TIRF experiments, we had to establish (a) whether transfection of the fluorescent peptide was enough to induce the generation of the DCVs or whether cotransfection of REST/DBD-GFP was still needed and (b) whether the fluorescent peptide was co-distributed with Sg2 in specific puncta spread in the superficial cell layer (Marchaland et al., 2008).

The results reported in Fig. 5 validated the use of NPY-mRFP as a marker of DCV exocytosis. In fact, in 18 out of 19 control living astrocytes cotransfected with GFP alone, the exogenous NPY-mRFP appeared predominantly concentrated within thin cisternae apparently spread at random in the cytoplasm, which in 13 cells, were accompanied by a few scattered puncta of various apparent sizes (~100–600 nm; Fig. 5 A). TIRF analysis demonstrated that none of these structures were included in the evanescent wave illumination layer (Fig. 5 B). Moreover, no images of exocytosis were induced when control astrocytes transfected with NPY-mRFP were stimulated with 5 µM ionomycin (unpublished data). The peculiar distribution of the exogenous NPY-mRFP in control astrocytes was not specific in the fluorescent peptide because labeled cisternae (accompanied in one third of the cells by a few puncta) appeared also in 33 out of 33 control astrocytes upon transfection with the DCV membrane protein phogrin coupled to mCherry (Fig. S2 A). Transfection into control astrocytes of Sg2-GFP induced only a weak response, which was concentrated in a few discrete puncta spread around the nucleus (Fig. S2 C). In this case, the puncta were also positive for the vital lysosome marker LysoTracker blue (Fig. S2 D), which in contrast, failed to label the DCVs induced by transfection of REST/DBD-GFP (not depicted). In conclusion, transfection of control astrocytes with fluorescent

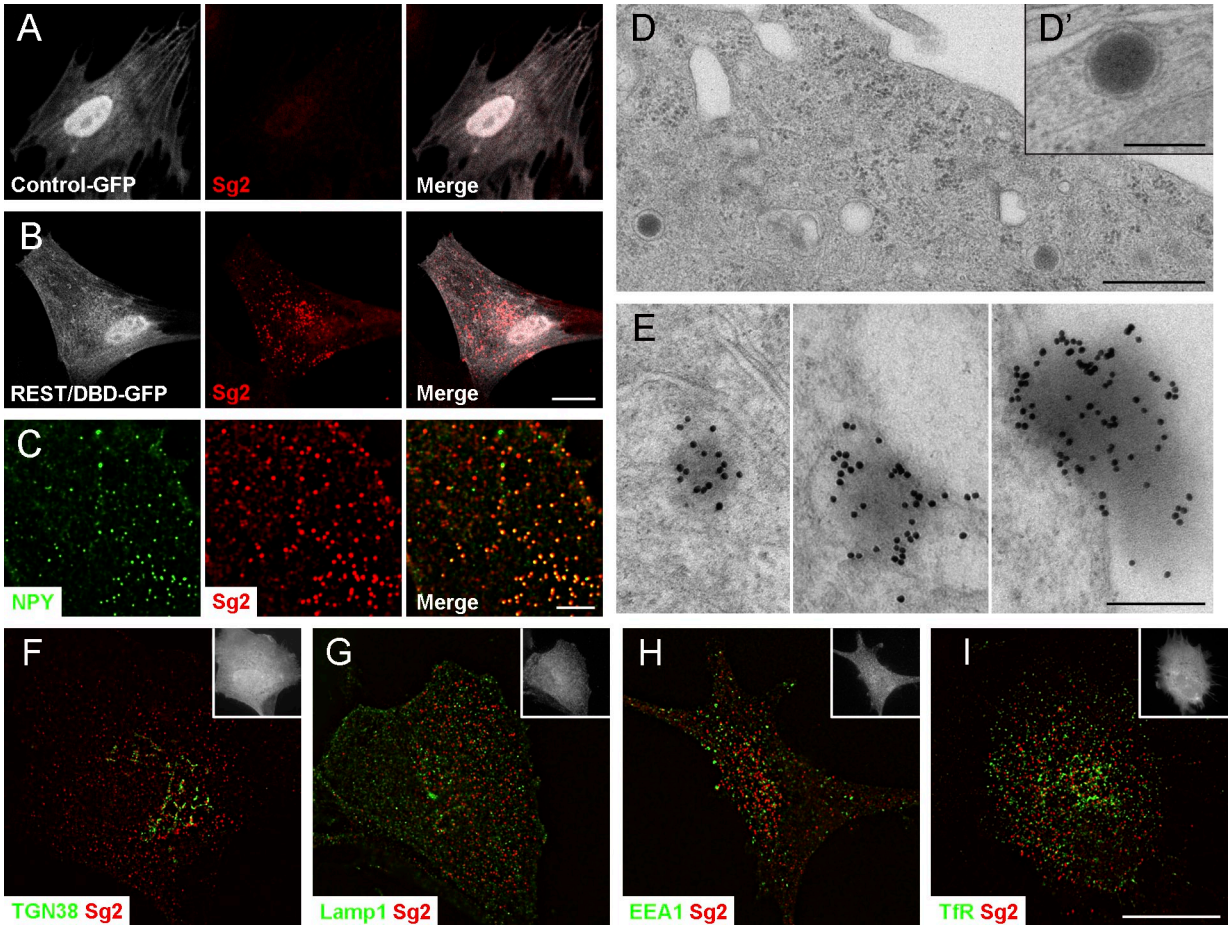

Figure 4. **Astrocytes transfected with REST/DBD-GFP express DCVs containing Sg2 and NPY.** (A and B) Representative confocal images of GFP and Sg2 compared in two transfected astrocytes. The control astrocyte (A) transfected with GFP remains negative for Sg2; the astrocyte transfected with the REST/DBD-GFP construct (B) also expresses the cargo protein concentrated in small puncta distributed preferentially in the perinuclear area and aligned in the proximity of the plasma membrane. (C) Most Sg2-positive puncta of REST/DBD-GFP–transfected astrocytes are also positive for the endogenous secretory peptide NPY. (D and D′) The conventional ultrastructure of DCVs expressed by the REST/DBD-GFP–transfected astrocytes. (E) Three DCVs, one deep in the cytoplasm, one adjacent to the surface, and one in the process of being exocytized, all strongly immunogold labeled for Sg2. (F–I) Astrocytes, all transfected with REST/DBD-GFP (see their GFP fluorescence in the insets) in which the distribution of Sg2 puncta does coincide only to a background level with those of the markers of TGN (TGN38; F), lysosomes (Lamp1; G), early endosomes (EEA1; H), and late endosomes (TfR; I). The images shown are representative of results obtained in at least three experiments. Bars: (A and B) 20 µm; (C) 5 µm; (D) 500 nm; (D′ and E) 200 nm; (F–I) 20 µm.

DCV markers (NPY-mRFP, phogrin-mCherry, and Sg2-GFP) induced accumulation within organelles (cisternae, a few puncta, and lysosomes) that appear distinct from exocytic DCVs.

The picture changed when astrocytes were transiently cotransfected with REST/DBD-GFP together with NPY-mRFP. In all these cells, mRFP fluorescence was concentrated in discrete puncta, ∼85% of which were also positive for Sg2, spread through the cytoplasm, and also present in the superficial layer of the cytoplasm (Fig. 5, C and E). The localization of non-DCV organelle markers in the specific NPY-mRFP–labeled small puncta was very low (Fig. S2, E–H). The pattern with small puncta was not typical of NPY-mRFP only because phogrin-mCherry–positive puncta predominated when the astrocytes were cotransfected with the membrane protein together with REST/DBD-GFP (Fig. S2 B). With exogenous NPY, however, the immunolabeling was not restricted to the puncta but was strong over parallel cisternae and heterogeneous puncta concentrated in the Golgi and trans-Golgi areas (Fig. S2, E–H), which were positive also for TGN38 and TfR, respectively (Fig. S2, E and H).

TIRF analysis confirmed, in the astrocytes cotransfected with REST/DBD-GFP and NPY-mRFP, the presence of superficial NPY-mRFP–positive puncta that are immobile or wondering around in the cytoplasmic layer illuminated by the evanescent wave (Fig. 5 D). Fluorescence of ∼60% of these puncta occupied from 5 to 8 pixels comparable with the red fluorescence of beads 200 nm in diameter (Fig. S3). The latter size is not far from the mean diameter of the DCVs measured by electron microscopy (Fig. 4 D). Collectively, the results confirm that in the REST/DBD-GFP–transfected rat astrocytes, the majority of the NPY-mRFP puncta in the evanescent wave illumination layer of the cytoplasm correspond to the DCVs positive for endogenous Sg2 and NPY as illustrated in Fig. 4 (B–E).

Astrocyte DCVs are competent for regulated exocytosis

TIRF analysis of cultured rat astrocytes doubly transfected for REST/DBD-GFP and NPY-mRFP revealed Ca^{2+}-dependent regulated exocytosis of NPY-positive DCVs upon addition of

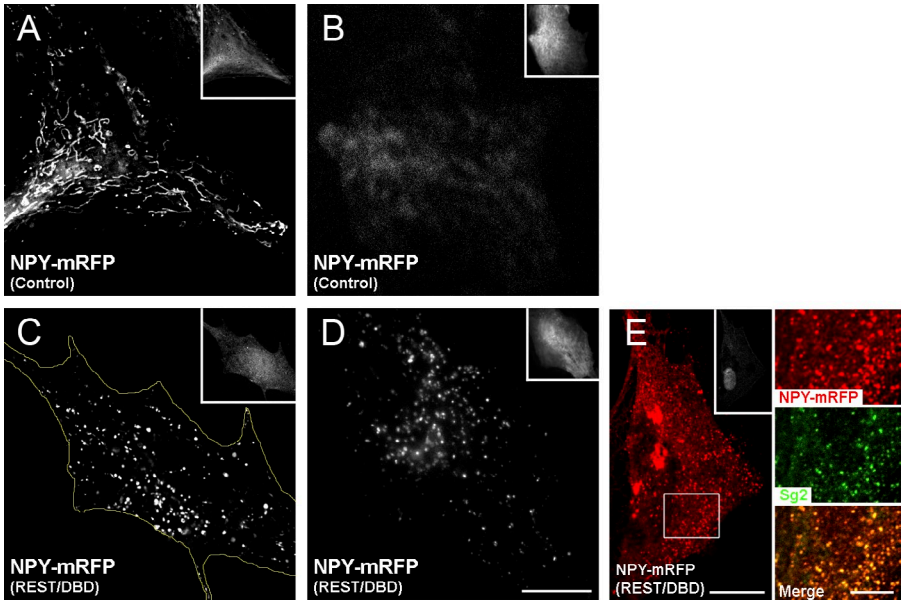

Figure 5. **Transfected NPY-mRFP is expressed into DCVs only in astrocytes cotransfected with REST/DBD-GFP.** The insets of all panels show the positivity of the cells for GFP (also positive for mRFP), documenting that they had been transfected with REST/DBD-GFP or the control construct. (A and B) In control cells, the distribution of NPY-mRFP is primarily in thin cisternae and few puncta (A, deconvolved image), which TIRF shows to be largely excluded from the surface layer of the cytoplasm illuminated by the evanescent wave (B). (C and E) In cells cotransfected with REST/DBD-GFP, NPY-mRFP is concentrated in scattered discrete puncta (C, deconvolved image) and colocalized with Sg2 (E, confocal image), corresponding, therefore, to the DCVs illustrated in Fig. 4 (D and E). The yellow line marks the contours of the cell. (D) Small NPY-positive puncta are abundant in the surface layer of the cytoplasm illuminated by the evanescent wave as illustrated by the TIRF image shown. The large fluorescent structures of E in the peri-Golgi area are accumulations of NPY-mRFP negative for Sg2 (not depicted; also see Fig. S2, E–H). The bottom box highlights the area of the three panels to the right showing the colocalization of NPY-mRFP and endogenous Sg2. A–E are representative of ≥10 cells produced in at least three transfection experiments. Bars: (A–E, left) 15 µm; (E, right) 5 µm.

5 µM ionomycin. The exocytic process was relatively slow, starting a few seconds after the application of the ionophore, reaching its maximum after 100 s, and continuing for ≤7–10 min, with a second smaller peak after 230 s (Fig. 6 A). The mean fluorescent fusions per cell were 26 ± 3. Fusions were specific because compared with seven control cells, their number decreased by almost 80% in five astrocytes pretreated for 2 h with BoNT/B and analyzed 20 h later (Fig. S4; Verderio et al., 1999). The fused puncta often evolved into fluorescent annuli that faded out within ∼500 ms (Fig. 6 B), a typical time course that documents the diffusion of the discharged NPY-mRFP cargo to the extracellular space.

In human brain cortex astrocytes, the levels of REST and DCV markers vary from very low to high

We next attempted to investigate by immunofluorescence whether DCVs, such as those described in cultured astrocytes transfected with REST/DBD-GFP (Fig. 4 and Fig. 5), are also present in situ in the tissue astrocytes. Our preliminary experiments of rat brain sections performed by the use of a few anti-REST commercial antibodies also used by others for immunofluorescence (Shimojo, 2008; Kohyama et al., 2010) yielded inconclusive results. The only anti-REST available to us that in human brain tissue sections, yielded signals of clearly different strength in the various cell types was a rabbit pAb obtained from Sigma-Aldrich raised against a peptide that was ∼50% different in the human and rodent RESTs. The specificity of this pAb was demonstrated in human NT2 cells in which REST had been knocked down by transfection with a construct containing GFP together with a specific small hairpin RNA (shRNA). Fig. S5 A shows that this transfection greatly reduced pAb immunolabeling (Sigma-Aldrich) of the REST-specific 225-kD Western blot band with respect to control NT2 cells transfected with a scrambled RNA–GFP construct.

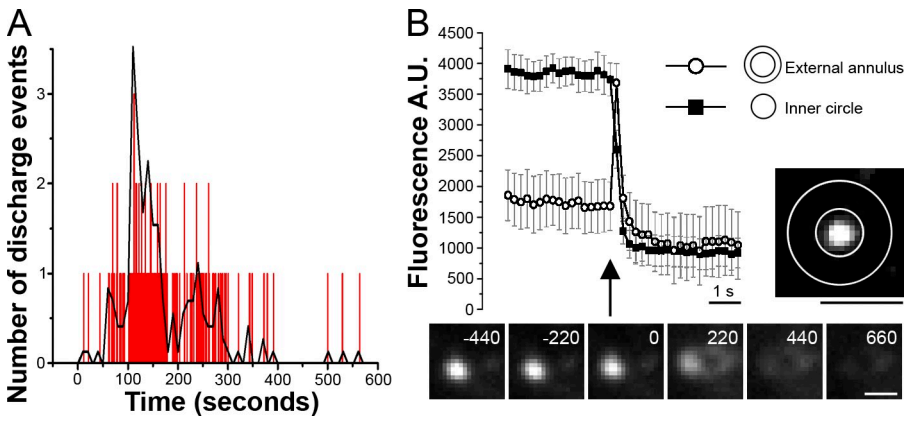

Figure 6. **DCVs undergo regulated exocytosis.** (A) The temporal distribution of the fusion events of NPY-mRFP–positive DCVs in astrocytes cotransfected with REST/DBD-GFP and treated with 5 µM ionomycin at time 0. Each individual histogram represents the number of fusion events detected during a 200-ms-long frame in eight astrocytes. Each point of the black line reports the number of discharge events occurring in 10 s. (B) The mean kinetics of the NPY-mRFP fluorescence intensity in the course of single-discharge events (n = 8). Upon fusion, the fluorescence of puncta (inner circles) fades out with the concomitant increase of fluorescence in the external annuli (see scheme on the right), which then rapidly dissolve. The image line on the bottom illustrates the subsequent steps of a typical discharge event. In this line, numbers are in milliseconds. Bars: (B, top) 2 µm; (B, bottom) 1 µm. A.U., arbitrary unit.

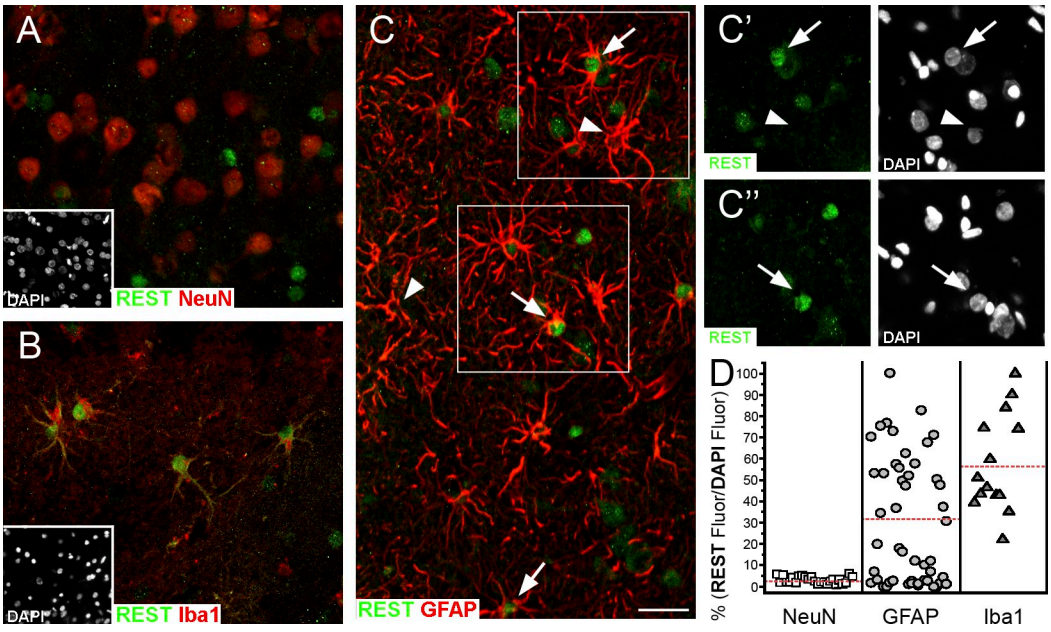

Figure 7. **Expression of REST in various cell types of the human brain temporal cortex.** All images (representative of six slices from two tissue samples) are z projections of stacks ~8-µm thick. The insets in A and B show the nuclei of all cells present in the panels labeled by DAPI. (A) Neurons labeled by the nuclear marker NeuN. Notice in these cells the lack of any appreciable nuclear REST labeling. All the green nuclei of this image belong to NeuN-negative nonneuronal cells. (B) Microglial cells immunolabeled in the cytoplasm for the marker Iba1. Notice that in all Iba1-positive cells, nuclei are strongly REST positive. (C) The variable expression of REST in the nuclei of astrocytes identified by the cytoplasmic marker GFAP. Some astrocytes exhibit a high REST labeling of the nucleus (arrows), whereas in others, the nuclear REST labeling is inappreciable (arrowheads). (C′ and C″) The areas boxed in C, documenting that the astrocyte nuclei present in the image are both positive (arrows) and negative (arrowheads) for REST, were similar in size and in DAPI fluorescence intensity. (D) Comparison, in quantitative terms, of the REST fluorescence of single nuclei in the three cell types, normalized to their DAPI fluorescence. The anti–human REST antibody used in this figure, in Fig. 8, and in Fig. S5 was the rabbit pAb from Sigma-Aldrich. The red lines mark the mean value of the REST/DAPI fluorescence ratios in the three cell types. (A–C″) Bar, 30 µm.

In rat astrocytes and PC12-27 cells, the Western blot immunodecoration with the anti–human REST pAb (Sigma-Aldrich) was completely lacking (see the comparison with positive human NT2 cells in Fig. S5 B, left), and no nuclear immunolabeling was observed in astrocytes of the rat brain cortex sections exposed to the same pAb (Fig. S5 B, right). We concluded that this pAb was appropriate to study the distribution of REST in fragments of the human cortex removed by neurosurgery and fixed immediately thereafter but not in cells of the rat.

Human brain fragments were first analyzed to validate their normal cellular structure. Sections of validated fragments were then investigated by immunofluorescence. In agreement with our subcellular fractionation results in astrocytes, PC12 (Fig. 1 C), and other cell types (not depicted), the REST of all human brain cells appeared to be concentrated almost exclusively in the nucleus. In neurons identified by the specific marker, neuronal nuclei (NeuN), the REST signal was very low or almost inappreciable (Fig. 7 A), whereas in microglial cells positive for the marker Iba1, it was strong (Fig. 7 B). In astrocytes positive for GFAP, REST immunofluorescence was variable, ranging from almost inappreciable to as high as in microglia (Fig. 7 C). A quantitative analysis of REST fluorescence in single nuclei normalized on DAPI fluorescence confirmed that low/inappreciable levels were common to all neurons and that the levels of microglia ranged from ~25 to 100% of the maximal REST/DAPI ratio observed. Among astrocytes, those showing almost inappreciable levels of REST were over one third. Those exhibiting higher values, which were lower, however, than the minimum of microglia, were ~15%. In the remaining ~50%, the REST levels were high, spread in the same range of microglia (Fig. 7 D).

Additional sections of human cortex tissue were immunostained for Sg2. Unfortunately, no dual Sg2/REST labeling could be made because, of the available antibodies against the granin, only a rabbit pAb (Calegari et al., 1999) yielded good results. In astrocytes, the levels of Sg2 distributed to the whole cytoplasm were quite variable (Fig. 8 A, arrow and arrowhead), with about half the cells being almost negative (Fig. 8 A″) and the rest showing signals of variable strengths, up to clearly positive values (Fig. 8 A′). Other astrocytes that were positive for GFAP were coimmunolabeled for NPY and REST (sheep and rabbit pAb's). Fig. 8 B shows that in a cell with high REST in the nucleus (Fig. 8 B, arrows), the cytoplasmic NPY was low, whereas in two cells with lower levels of REST (Fig. 8 B, arrowheads), the NPY signal was stronger. A similar inverse correlation was observed in a total of 64 cells. However, the NPY data could not be appropriately quantitated because of the presence of strongly positive synapses overlapping the astrocyte cytoplasm. Collectively, these data suggest that the heterogeneous levels of REST are responsible, at least in part, for the variable expression of gliosecretion in human astrocytes. The REST/neurosecretion link of human astrocytes remains, however, to be characterized in further detail.

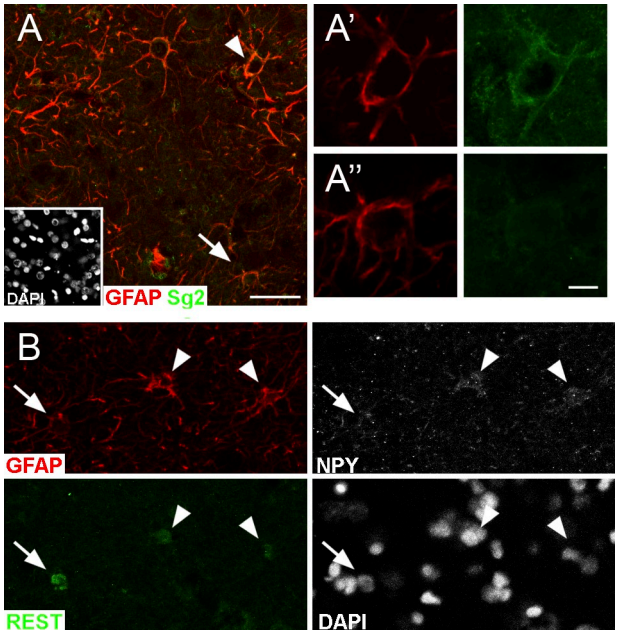

Figure 8. **Variable expression of Sg2 and NPY in GFAP-positive astrocytes of the human brain temporal cortex.** All images are z projections of stacks ~8 (A and B)- and 4 (A′ and A″)-µm thick. The inset in A shows the DAPI fluorescence of the nuclei in the figure. (A–A″) The levels of Sg2 in the GFAP-positive astrocytes vary considerably from high (arrowhead; see the zoom in A′) to low (arrow; see the zoom in A″). (B) The triple immunolabeling of a few astrocytes identified by their positivity for GFAP that exhibit variable levels of REST and NPY (gray). Notice that the cell with high REST in the nucleus (arrows) shows a weak NPY signal in the cytoplasm, whereas two cells with lower REST (arrowheads) show higher signals for the peptide. Bars: (A and B) 30 µm; (A′ and A″) 5 µm.

Discussion

The role of REST in the expression and regulated exocytosis of DCVs had been previously investigated in two nerve cell types known to express the organelles, pheochromocytoma PC12 cells, and brain neurons. In PC12, a strict dependence was demonstrated conclusively (Bruce et al., 2006; D'Alessandro et al., 2008), and in neurons, it appears quite likely. In fact, various proteins involved in DCV composition and discharge are directly repressed by REST (Schoenherr et al., 1996; Ballas and Mandel, 2005; Ekici et al., 2008), whereas others are candidates of repression because their genes exhibit, in their regulatory domains, one or a few copies of RE-1, the DNA-binding sequence of REST (Bruce et al., 2004; Mortazavi et al., 2006; Otto et al., 2007). Decreases of REST or expression of truncated forms accompanied by expression of a few neurosecretion genes was found to also take place in aggressive forms of nonnerve cell tumors of the breast, lung, colorectum, and prostate (Coulson, 2005; Westbrook et al., 2005; Wagoner et al., 2010). In these tumors, however, morphological and functional studies have not been performed yet. Whether the expression of neurosecretion markers is accompanied or not by the appearance of DCVs discharged by regulated exocytosis is, therefore, still unknown.

In astrocytes, the role of REST had been investigated in only two recent papers (Abrajano et al., 2009; Kohyama et al., 2010), neither of which was interested in gliosecretion. Therefore, the possibility of a REST dependence for the process remained to be investigated. In agreement with Kohyama et al. (2010), we have found the levels of REST to be high in cultured astrocytes. In these cells, therefore, processes dependent on REST should all be repressed. Yet, studies from many laboratories, including ours (Bezzi et al., 2004; Volterra and Meldolesi, 2005; Domercq et al., 2006; Marchaland et al., 2008), had shown cultured astrocytes to be fully competent for CV gliosecretion, i.e., to express CVs loaded with glutamate and exocytized upon stimulation (Haydon and Carmignoto, 2006; Parpura and Zorec, 2010). CV gliosecretion may therefore be independent of REST. In contrast, the studies of DCVs yielded variable results. The expression of these vesicles had been reported in cultured astrocytes >10 yr ago by Calegari et al. (1999). More recently, DCVs were shown to undergo regulated exocytosis, with the release of their cargo peptides (atrial natriuretic peptide and NPY) and ATP (Kreft et al., 2004; Pangrsic et al., 2007; Ramamoorthy and Whim, 2008). However, all astrocytes from the present work, which were isolated and cultured according to an established procedure (Bezzi et al., 2001), were found to exhibit neither DCVs nor their markers. Moreover, when transfected into our astrocytes, Sg2-GFP was targeted to lysosomes, whereas NPY-mRFP and the DCV membrane protein phogrin-mCherry did not accumulate primarily in exocytic organelles but in numerous thin cisternae that remain to be identified. A REST control of the DCV expression and of their gliosecretion appeared therefore possible.

The first indication that was consistent with this type of control came from the characterization of our astrocyte cultures that were negative for DCVs, Sg2, and a variety of other proteins involved in neurosecretion, all encoded by genes sensitive to REST (D'Alessandro et al., 2008). Only two SNAREs, VAMP2 and Stx1a, whose genes are little sensitive to REST (D'Alessandro et al., 2008), were expressed in our astrocytes. This picture changed when the repressive tone of REST was attenuated by the transient transfection of its dominant-negative construct, REST/DBD-GFP, which did not affect the nature of the cells documented by three astrocyte markers but induced the appearance of DCVs. Interestingly, not all proteins related to the organelles increased but only a few. Of the two t-SNAREs, Stx1a increased only slightly, whereas SNAP25 increased considerably, remaining, however, at a much lower level (~2%) compared with wtPC12 cells. Sg2 reached a higher value (~8% of wtPC12). In PC12-27 cells stably transfected with the REST/DBD-GFP construct, the same three proteins were also increased. However, the rise of Stx1a was 12-fold, whereas that of Sg2 was only twofold (D'Alessandro et al., 2008). These differences document the cell specificity of the REST control of gene expression already reported by Belyaev et al. (2004) and Hohl and Thiel (2005).

As previously demonstrated in other cell types (Tooze, 1998; Day and Gorr, 2003; Huh et al., 2003; Malosio et al., 2004), the increase of Sg2 appeared necessary, but not sufficient, for the concomitant appearance of astrocyte DCVs, which occurred only upon attenuation of the REST tone. In fact, the puncta generated upon transfection of the granin alone were not DCVs but lysosomes. In contrast, in the cells transfected with REST/DBD-GFP, the Sg2-positive puncta distributed, in part,

near the plasma membrane exhibited the typical ultrastructure and a mean diameter (~170 nm) within the span of nerve cell DCVs. Additional evidence for the DCV nature of these organelles included their positivity for an endogenous secretory peptide, NPY, and for a DCV membrane protein, phogrin, together with their negativity for markers of the TGN, endosomes, and lysosomes.

The final proof for the identification of the Sg2-positive puncta as astrocyte DCVs came from the TIRF analysis of the cells cotransfected with REST/DBD-GFP and NPY-mRFP. The number of puncta scattered in the superficial evanescent wave illumination layer of the cytoplasm that were discharged in response to the Ca^{2+} rise was not large (26 per cell on average). However, discharge was significant and specific because it was largely prevented by pretreatment of the cells with BoNT/B. The kinetics of the process was much slower than that of astrocyte CVs (Bezzi et al., 2004; Calì et al., 2008) but analogous to that previously reported by Pangrsic et al. (2007) studying DCV gliosecretion of ATP. Collectively, our data confirm that in astrocytes, the expression of DCVs and their discharge are governed at the transcriptional level by REST, the same factor that governs expression of neurosecretion in nerve cells. In our cultured astrocytes, DCV gliosecretion required the REST tone to be decreased. Our hypothesis is that a REST tone comparable with that of our astrocytes transfected with REST/DBD-GFP is present, even without transfection, in the astrocytes cultured in other laboratories that were reported to exhibit DCVs.

The heterogeneity of REST levels in human brain tissue astrocytes was unexpected. In view of the specificity of the only anti-REST pAb that yielded convincing immunocytochemical results, our experiments could be performed only in human brain cortex fragments removed during neurosurgery. Neurons and microglia were found to exhibit different levels of REST: the first was very low/inappreciable, and the second was high (variability was less than fourfold). In contrast, astrocytes identified by their marker GFAP did span the whole range of the observed REST values: over one third were as low as neurons, and ~15% was still low but higher than neurons; the remaining 50% was as high as the microglia. Heterogeneities in size, shape, receptors, proteins, and, most likely, also function are well-known properties of astrocytes (Wilhelm et al., 2004; Volterra and Meldolesi, 2005; Oberheim et al., 2006; Wang and Bordey, 2008; Hewett, 2009; Matyash and Kettenmann, 2010). REST is known to repress the transcription of hundreds of target genes (Bruce et al., 2004; Mortazavi et al., 2006; Otto et al., 2007), however, with different sensitivity (D'Alessandro et al., 2008). Moreover, additional effects of the repressor are induced indirectly (Ballas and Mandel, 2005; Ooi and Wood, 2007; Abrajano et al., 2009). Therefore, at least some of the astrocyte heterogeneities could be caused by differences in their REST levels. However, many astrocytes with different phenotypes have a specific localization: in the gray and the white matter, the retina, the cerebellum, and so on. In the only brain tissue we have investigated, the human cortex, we have found intermixed astrocytes with different REST expression. A reason for this REST heterogeneity could be functional. Because of its fast turnover ($t_{1/2}$ = 40 min; Westbrook et al., 2008) REST can change its levels rapidly (Guardavaccaro et al., 2008). Depending on their signaling state, astrocytes might be able to adjust their expression of REST with ensuing changes, among other properties, of their DCV gliosecretion. Our results for Sg2 and NPY immunolabeling might be suggestive in this direction. We found that the levels of Sg2 are also variable among astrocytes of the human cortex, with ~50% looking positive and ~50% low or negative for the granin. With NPY, we found that cells rich in REST were poor in the peptide and vice versa. However, a final demonstration of this negative correlation will need further dual-labeling studies with new antibodies.

In conclusion, our results in astrocytes have shown that DCVs and their gliosecretion are expressed under the control of REST, apparently at variance with the CVs of the same cells. In the human brain cortex, astrocytes exhibit a unique heterogeneity in REST expression, ranging from levels as low as those of neurons to levels as high as those of microglia. These properties should be taken into consideration to explain conflicting results reported in the literature in this area. In the expanding framework of astrocyte functions and in view of the key role of REST in the expression of hundreds of genes, our results might, ultimately, be useful to explain mechanisms that are operative not only in the expression and function of DCVs but also in other aspects of brain physiology and, possibly, also of its pathology.

Materials and methods

Reagents and antibodies

The anti-Sg2 rabbit pAb (Calegari et al., 1999) was a gift from P. Rosa (National Research Council Institute of Neuroscience, Milan, Italy); BoNT/B was a gift from O. Rossetto (University of Padova, Padova, Italy); and anti–rat ChgB mAb was developed in our laboratory (Borgonovo et al., 2002). Other antibodies were obtained from the following sources: anti-REST and anti-H2b pAb's were obtained from Millipore; anti-REST mAb 12C11-1 was a gift from David J. Anderson (California Institute of Technology, Pasadena, CA); anti–human REST rabbit HPA006079 pAb, anti GFAP mAb, and anti–β-tubulin mAb were purchased from Sigma-Aldrich; anti-ChgA mAb was purchased from Thermo Fisher Scientific; anti-Rab3a, anti-Stx1a, anti-Syt1, anti-Syp, and anti-VAMP2 mAb's and anti-Munc18, anti-Syt4, and anti-SNAP23 rabbit pAb's were obtained from Synaptic Systems; anti-SNAP25 mAb was obtained from Covance; anti-S100β rabbit pAb was purchased from Dako; anti-NPY sheep pAb, anti-GFAP, anti-NeuN, and anti-GS mAb's were obtained from Millipore; anti-TGN38 mAb was obtained from Thermo Fisher Scientific; anti-Lamp1 and anti-EEA1 mAb's were purchased from BD; anti-TfR mAb was obtained from Invitrogen; anti-VAMP3 rabbit and anti-Iba1 goat pAb's were obtained from Abcam; horseradish peroxidase–conjugated goat anti–mouse and anti–rabbit pAb's were purchased from Bio-Rad Laboratories; FITC-conjugated anti-GFP pAb was obtained from Novus Biologicals; FITC-conjugated, TRITC-conjugated, and CY5-conjugated goat anti–mouse and goat anti–rabbit pAb's were obtained from SouthernBiotech; Alexa fluor 488–conjugated, Alexa fluor 555–conjugated, and Alexa fluor 647–conjugated goat anti–mouse, goat anti–rabbit, donkey anti–mouse, donkey anti–rabbit, and donkey anti–sheep pAb's were obtained from Invitrogen; and 15-nm colloidal gold particles coated with anti–rabbit IgG were obtained from BB International. The BCA Protein Assay kit was purchased from Thermo Fisher Scientific; BSA was obtained from Roche; Lipofectamine 2000, LysoTracker blue, and carboxylate-modified microspheres (FluoSpheres) were purchased from Invitrogen; London Resin white was obtained from EMS; PBS was obtained from Euroclone; and ionomycin, Epon, DAPI, goat normal serum, donkey normal serum, and all other chemicals were purchased from Sigma-Aldrich.

The pAdTrack-CMV-GFP (control-GFP) and the pAdTrack-CMV-REST/DBD-GFP (REST/DBD-GFP) constructs were gifts from N.J. Buckley (King's College, London, England, UK); the NPY-mRFP construct was a gift from R. Regazzi (University of Lausanne, Lausanne, Switzerland); and the Sg2-GFP construct was a gift from M. Courel (University of Rouen, Mont-Saint-Aignan, France). Rat phogrin (available from GenBank/EMBL/DDBJ under

accession no. Z50735) was cloned with EcoRI–AgeI into the pmCherry-N1 vector (gift from M. Iezzi, University of Lausanne, Lausanne, Switzerland). The REST/NRSF target sequence used to design its shRNA was 1,032 5′-ACATGCAAGACAGGTTCACAA-3′, which was identified by using an RNAi designer algorithm (BLOCK-iT; Invitrogen). The shRNA construct was obtained by cloning the 1,032 sequence into pcDNA 6.2-GW/EmGFP-miR using an RNAi expression vector kit (BLOCK-iT Pol II miR; Invitrogen) according to the manufacturer's instructions. As a negative control, we used the pcDNA 6.2-GW/EmGFP-miR-neg plasmid containing a sequence targeting any known vertebrate gene. Both plasmids were gifts from D. Pozzi (San Raffaele Scientific Institute, Milan, Italy).

Buffers

Lysis buffer (LB) contained 1% Triton X-100, 50 mM Tris-HCl, pH 7.5, 250 mM NaCl, 5 mM EDTA, and protease inhibitor cocktail (Sigma-Aldrich). For cytoplasmic and nuclear protein extraction, buffer A consisted of 10 mM Hepes-KOH, pH 7.8, 1.5 mM $MgCl_2$, 10 mM KCl, 0.5 mM DTT, and protease inhibitor cocktail; buffer B consisted of 0.3 M Hepes-KOH, pH 7.8, 1.4 M KCl, 30 mM $MgCl_2$, and protease inhibitor cocktail; and buffer C consisted of 20 mM Hepes-KOH, pH 7.8, 25% glycerol, 0.42 M NaCl, 1.5 mM $MgCl_2$, 0.2 mM EDTA, 0.5 mM DTT, and protease inhibitor cocktail. Sucrose was dissolved in 5 mM Hepes, pH 7.3. TBS with Tween (TBST) consisted of 200 mM NaCl, 50 mM Tris, pH 7.4, and 0.05% Tween 20. Hepes–Krebs-Ringer Hepes (KRH) contained 120 mM NaCl, 3.1 mM KCl, 2 mM $MgCl_2$, 1.8 mM $CaCl_2$, 1.25 mM NaH_2PO_4, 25 mM Hepes-Na, pH 7.4, and 4 mM glucose. Radioimmunoprecipitation assay (RIPA) buffer consisted of 1 mM NaEDTA, 0.5 mM NaEGTA, 10 mM Tris-HCl, pH 8, 1% Triton X-100, 0.1% Na-deoxycholate, 0.1% SDS, 140 mM NaCl, and 1 mM PMSF. The phosphateglycine buffer was made of phosphate buffer and 0.1 M glycine.

Cell cultures

All cells were grown at 37°C in 5% CO_2. Primary astrocytes were obtained from 1-d-old Sprague-Dawley rat pups (Charles River and Janvier) sacrificed according to procedures approved by the Issues for Institutional Animal Care and Use Committees of the San Raffaele Institute and the Swiss Federal Veterinary Office. Freshly dissected cerebral cortices were disaggregated mechanically, washed, and seeded. After 10–14 d, they were depleted of microglial cells by shaking and seeded again for 1–2 d in MEM (Sigma-Aldrich) with 10% horse calf serum (PAA Laboratories), 2 mM glutamine, 100 U/ml penicillin and streptomycin (PAA Laboratories), and 0.3% glucose. For further details see Bezzi et al. (2001). Rat pheochromocytoma wtPC12 and PC12-27 clones (as in Borgonovo et al., 2002) were grown in DME (Lonza) with 10% horse serum (Euroclone) and 5% fetal clone III serum (Hyclone Laboratories) supplemented with 2 mM ultraglutamine and 100 U/ml penicillin and streptomycin (Lonza). Human teratoma NT2 cells were grown in DME with 10% fetal clone III serum supplemented with 2 mM ultraglutamine and 5 U/ml penicillin and streptomycin.

Transfections

Plasmids containing NPY-mRFP, phogrin-mCherry, Sg2-GFP, GFP alone, or REST/DBD-GFP (1.8 µg for single transfections; 1 µg each for double transfections) were transfected into primary rat cortical astrocyte cultures by Lipofectamine 2000. Cells were analyzed 24–48 h after transfection. In some experiments, transfected astrocytes were sorted out from negative cells by FACS plus (BD). The shRNA constructs were transfected in human NT2 cells by the Lipofectamine 2000 technique.

mRNA isolation and quantitative RT-PCR

Total cellular RNAs extracted according to the RNeasy Mini kit (QIAGEN) were used for reverse transcription according to a first-strand synthesis system (SuperScript III; Invitrogen). The synthesized cDNAs were templates for quantitative PCR (Taqman) performed by the RT-PCR and DNA sequencing service of the Istituto Fondazione Italiana Ricerca sul Cancro di Oncologia Molecolare–Istituto Europeo di Oncologia Campus for Oncogenomics (IFOM-IEO). 18S RNA was used for normalization. Rqmin/Rqmax indicates the SEM (confidence 95%), in which Rqmin/Rqmax is the ratio between the minimal and maximal relative quantification of a nucleic acid sequence in a test sample (Fig 1 A and Fig. 3 A).

Chromatin immunoprecipitation

Astrocyte chromatin was prepared from cultured astrocytes cross-linked with 1% formaldehyde for 10 min and then treated with 10 sonication cycles of 35 s at 60–70 W (Ultrasonic Processor XL Sonicator; Miosonix), each followed by a 2-min rest on ice. Cross-linked chromatin-containing fractions (Klajn et al., 2009) were pooled and stored at −80°C. 20-µg aliquots were precleared with 35 µl protein A–Sepharose-coated beads (Pharmacia) in RIPA buffer and split in three. Each aliquot was then incubated overnight with 1 µg anti-REST, 1 µg anti-VAMP3 (negative control), or without antibodies (mock controls) in a total volume of 1 ml RIPA buffer. After immunoprecipitation, the material was treated with 50 µg/ml RNaseA for 30 min at 37°C and by 500 µg/ml proteinase K in 0.5% SDS at the same temperature overnight. Cross-links were reverted by heating the samples at 65°C for 5 h. The purified DNA was resuspended in 60 µl of distilled water, and 6-µl aliquots were used as a template. The chromatin immunoprecipitation–enriched DNAs of the indicated amplicon (SNAP25) were quantified by quantitative PCR in a light cycler (LC480; Roche) using a DNA mix SYBR green I kit (FastStart; Roche). The values subtracted of the mock values, given in Fig. S1, are means of three separate experiments ± SD. For further details see Klajn et al. (2009).

Subcellular fractionation and protein extracts

Total cell extracts were obtained by washing cells in PBS and solubilizing them in LB. Samples were rocked at 4°C for 15 min and then centrifuged at 13,000 *g* at 4°C for 15 min to recover the postnuclear supernatant. Nuclear and cytoplasmic fractions were separated by gradient centrifugation according to Dignam et al. (1983). Cells were washed in PBS, collected by scraping on ice, and centrifuged for 5 min at 900 rpm at 4°C. Pellets were resuspended in 5 vol buffer A supplemented with 0.3% Triton X-100. After 30 s of vortexing and centrifugation for 1 min at 11,000 rpm at 4°C, the supernatants were added with 1/10 vol buffer B, incubated for 15 min at 4°C, and centrifuged at 14,000 rpm for 15 min to remove contaminants; the pellet was resuspended in 1.6 M sucrose. 300 µl of resuspended nuclei were transferred to the bottom of a centrifuge tube and covered with 450 µl of 1.5-M sucrose and then with 450 µl of 0.32-M sucrose. After centrifugation in a swing bucket rotor at 100,000 *g* for 1 h at 4°C, the pellet was resuspended in 20 µl buffer C, incubated for 15 min at 4°C, and centrifuged for 15 min at 14,000 rpm to clear the supernatant. Protein concentration was determined by the bicinchoninic acid assay.

Western blotting

Equal amounts of proteins (20–50 µg) were separated by SDS-PAGE and then transferred to nitrocellulose filters. After blocking for 1 h at RT with 5% nonfat dry milk in TBST, the filters were incubated for 2 h at RT or, alternatively, overnight at 4°C with primary antibodies diluted in TBST, 1% BSA, and 0.02% sodium azide and then washed five times for 10 min in TBS, incubated for 1 h at RT with the appropriate peroxidase-conjugated secondary antibodies (1 µg/ml) in 5% nonfat dry milk in TBST, and washed again in TBST five times for 10 min. Photographic development was by chemiluminescence (ECL [GE Healthcare]; Immobilon Substrate [Millipore]). Western blot bands were quantified by the ImageJ program (National Institutes of Health). The data presented, which are expressed as a percentage of the corresponding values in wtPC12 cells, are means of at least three experiments ± SD.

Living cell image acquisition

Cultured astrocytes cotransfected with either the control-GFP or the REST/DBD-GFP constructs together with NPY-mRFP, phogrin-mCherry, or Sg2-GFP constructs seeded on 24-mm-diameter coverslips were placed in an appropriate chamber and incubated in Hepes-KRH at 37°C. Optical sections were taken with a 100×/NA of 1.4 Plan Apochromat oil objective (Olympus) every 150 nm with a wide-field microscope (IX70; Olympus) equipped with an RT Deconvolution system (DeltaVision). Images were acquired with a camera (CoolSnap HQ^2; Roper Scientific) and deconvoluted with the softWoRx Deconvolve software (Applied Precision) to remove the blur in fluorescence (as in Borgonovo et al., 2002).

Immunofluorescence of cultured astrocytes

Transfected astrocytes seeded on 24-mm-diameter coverslips were fixed on ice for 10 min with 4% paraformaldehyde in PBS. After repeated washes in PBS, they were incubated for 1.5 h at RT with primary antibodies in PBS, 1% BSA, and 0.2% Triton X-100 or 0.4% saponin depending on the antigens. Cells were then extensively washed in PBS, exposed to fluorescent conjugated secondary antibodies in PBS and 1% BSA for 1 h at RT, washed again, incubated with DAPI for 5 min, and finally, mounted with a reagent (FluorSave; EMD). Analyses were performed at RT in a laser confocal microscope (TCS SP2; Leica) with a Plan Apochromat 63×/NA of 1.4 oil objective. Alternatively, optical sections taken every 150 nm with a wide-field microscope (IX70) with a RT Deconvolution system were deconvolved as in the previous paragraph. Wide-field images were rendered using softWoRx Deconvolve software and ImageJ; confocal images were rendered

using confocal software (LCS Lite; Leica). Illustrations were prepared using Photoshop software (Adobe). Background subtraction and scaling were performed using nonsaturated images and linear lookup tables.

Immunohistochemistry of rat and human brain cortex tissue slices

Living rats anesthetized with an intraperitoneal injection of 50 mg/kg pentobarbital were perfused intracardially with 4% paraformaldehyde. The brain was extracted and washed in PBS. Fragments of normal structure from human brain temporal cortices were removed as part of the planned margin of resection surrounding a neoplastic lesion from patients operated at the Section of Neurosurgery in the Policlinic San Matteo. Surgery was performed according to the recommendations of the Institutional Review Boards and in full agreement with the Declaration of Helsinki. Samples were fixed in 4% formaldehyde for 24 h and then washed in PBS.

Upon fixation and washing, all samples were immersed overnight in 30% sucrose at 4°C for cryoprotection and then plunged in isopentane and cooled to −40°C for 1 min for rapid freezing. 30-µm-thick slices were cut in a cryostat (CM 1800; Leica) and placed on glass slides that were kept at −80°C.

Immunolabeling of slices was performed at RT after three washes in PBS for 10 min and permeabilization for 45 min in PBS, 0.3% Triton X-100, and 15% donkey or goat serum. After three more washes in PBS for 10 min, the slices were incubated overnight at 4°C with primary antibodies in PBS, 0.1% Triton X-100, and 1.5% serum. The day after, samples were washed again three times in PBS for 10 min and incubated for 1.5 h at RT with secondary antibodies diluted in PBS and then washed again and exposed to DAPI for 10 min before mounting with a reagent (FluorSave). Labeled slices were analyzed at RT in a laser confocal microscope (TCS SP5) with a Plan Apochromat 40×/NA of 1.4 oil objective. Sections were acquired every 0.4-µm thickness, and confocal images were rendered using confocal software (LAS AF Lite; Leica). Illustrations were prepared using ImageJ and Photoshop software. Cells costained for REST, specific markers, and DAPI were selected manually, and nuclei were analyzed quantitatively for fluorescence intensity by ImageJ software. Data from each single nucleus normalized on its DAPI staining are given as a percentage of the maximum observed value in the whole cell population.

Electron microscopy

Low speed centrifugation pellets of REST/DBD-GFP–transfected, FACS–enriched astrocytes were fixed with 4% formaldehyde plus 2.5% glutaraldehyde in phosphate buffer, washed, postfixed in 2% OsO_4 in phosphate buffer, and embedded in Epon. For immunogold labeling, cells were fixed with a 4% formaldehyde–0.25% glutaraldehyde mixture in phosphate buffer, extensively washed, and embedded in London Resin white. Ultrathin sections on nickel grids were exposed to the anti-Sg2 for 90 min in phosphateglycine buffer, washed, immunolabeled with 15-nm gold particles coated with anti–rabbit IgGs, washed, postfixed with 1% glutaraldehyde, and finally stained in sequence with uranyl acetate and lead citrate. Controls were ultrathin sections of control-GFP–transfected astrocytes processed as the REST/DBD-GFP–transfected astrocytes. 60-nm ultrathin sections were studied and photographed in an electron microscope (Leo 912 AB; Carl Zeiss). Radii of DCVs were measured on digital images. Corrections of the radius measurements were made as in Parsons et al. (1995).

Astrocyte cultures for imaging experiments

Astrocytes obtained from newborn pups essentially as previously described (Bezzi et al., 2004; Domercq et al., 2006) were plated (2.5×10^4 cells) on glass 24-mm-diameter coverslips and transfected 1–2 d later with the NPY-mRFP with or without the REST/DBD-GFP or the control-GFP constructs. 2 d after transfection, coverslips were mounted in the open laminar flow perfusion incubator (SA-20LZ; Harvard Apparatus) on the stage of a fluorescence inverted microscope (Axiovert 200; Carl Zeiss) modified for TIRF and epillumination (EPI) experiments (Visitron System). The 250-µl volume experimental chamber was perfused at a rate of 1–1.5 ml/min at 30–32°C with a Hepes-KRH buffer. 5 µM ionomycin was applied rapidly by means of a pipette. In some experiments, cells were treated with 90 nM BoNT/B for 2 h in KRH. Control cells were incubated in plain KRH according to Verderio et al. (1999). After washing, the incubation was pursued in complete culture medium for 20 h to allow proteolytic cleavage of the substrate.

Optical imaging

For TIRF illumination imaging experiments, the expanded beam of a 488/568-nm argon/krypton multiline laser (20 mW; Laserphysics) passed through a laser wavelength selector (AOTF; VisiTech International) synchronized with a charge-coupled device camera (SNAP-HQ; Roper Scientific) under control of Metafluor software (Universal Imaging) was introduced to the coverslip from the high NA objective lens (1.45 NA; α-Plan Fluar 100×; Carl Zeiss). Light entered the coverslip and underwent total internal reflection at the glass–cell interface. In our experimental conditions, penetration depth of TIRF illumination was calculated to be 92 nm (Calì et al., 2008; Marchaland et al., 2008). In the TIRF/EPI illumination imaging protocol used in our experiments, EPI was generated by a polychromator illumination system (excitation light of 488 nm; Visichrome; Visitron). Once the GFP-expressing cell was recognized, TIRF illumination (excitation of 568 nm) was switched on. The pixel size was 126 nm.

TIRF analysis

The dynamics of individual NPY puncta was studied in TIRF experiments by monitoring the mRFP fluorescence in a 1.25-µm-diameter circle positioned on top of the spot and in a concentric annulus (inner diameter of 1.25 µm; outer diameter of 2.5 µm; Zenisek et al., 2002; Bezzi et al., 2004). Fusion events were recognized as the series of stereotyped fluorescence changes illustrated in Fig. 6 B; just after the fusion event, the bright mRFP fluorescence spread to finally disappear. The temporal distribution of fusion events was obtained by plotting them against time. In all experiments, counting of fusion events was continued for ∼600 s from ionomycin application. To evaluate the pool of NPY DCVs resident in the evanescent field of illumination, cells expressing NPY-mRFP, which were visualized by 568-nm TIRF illumination, were manually selected and analyzed for their morphology (Fig. 5 E).

Statistical analysis

The significance of differences between pairs of mean values was assessed using the two-tailed unpaired *t* test. $P < 0.05$ is considered significantly different. In the figures, double asterisks indicate $P < 0.01$, and a single asterisk indicates $P < 0.05$.

Online supplemental material

Fig. S1 demonstrates that in cultured astrocytes, REST is associated to its target gene encoding the t-SNARE SNAP25. Fig. S2 demonstrates that the transfected DCV membrane protein phogrin-mCherry exhibits a different distribution in cultured astrocytes before (cisternae) and after (discrete puncta) cotransfection of REST/DBD-GFP. Fig. S3 shows that in REST/DBD-GFP–transfected astrocytes, the mean radial sweep of the NPY-mRFP–positive puncta does not differ from that of red fluorescent beads 200 nm in diameter. Fig. S4 shows that the NPY-mRFP–positive fusions induced in astrocytes cotransfected with REST/DBD-GFP by ionomycin are decreased >80% upon preincubation with BoNT/B. Fig. S5 shows that the REST Western blot band of human astrocytes is almost completely abrogated upon shRNA knockdown of the repressor, documenting the specificity of the anti-REST antibody used. Online supplemental material is available at http://www.jcb.org/cgi/content/full/jcb.201010126/DC1.

We are grateful to Daniele Zacchetti for his precious advice in the initial part of this work; to Corrado Calì for TIRF analyses; to Julien Gremion and Gabriella Racchetti for experimental support; to Patrizia Rosa, Maite Courel, Noel J. Buckley, and Romano Regazzi for the gifts of antibodies and/or constructs; Mariella Iezzi for the generation of the phogrin-mCherry construct; Davide Pozzi for the generation of the REST shRNA constructs; and Ornella Rossetto for the BoNT/B.

The work was supported by grants from the Italian Institute of Technology and Telethon 2009 (GGP09066) to J. Meldolesi and from the University of Lausanne (FBM2006), the Foundation Novartis (26077772), and the Swiss National Foundation (National Centres of Competence in Research–Transcure) to P. Bezzi.

Submitted: 25 October 2010
Accepted: 1 April 2011

References

Abrajano, J.J., I.A. Qureshi, S. Gokhan, D. Zheng, A. Bergman, and M.F. Mehler. 2009. Differential deployment of REST and CoREST promotes glial subtype specification and oligodendrocyte lineage maturation. *PLoS ONE*. 4:e7665. doi:10.1371/journal.pone.0007665

Araque, A., and M. Navarrete. 2010. Glial cells in neuronal network function. *Philos. Trans. R. Soc. Lond. B Biol. Sci.* 365:2375–2381. doi:10.1098/rstb.2009.0313

Araque, A., V. Parpura, R.P. Sanzgiri, and P.G. Haydon. 1999. Tripartite synapses: glia, the unacknowledged partner. *Trends Neurosci.* 22:208–215. doi:10.1016/S0166-2236(98)01349-6

Ballas, N., and G. Mandel. 2005. The many faces of REST oversee epigenetic programming of neuronal genes. *Curr. Opin. Neurobiol.* 15:500–506. doi:10.1016/j.conb.2005.08.015

Belyaev, N.D., I.C. Wood, A.W. Bruce, M. Street, J.B. Trinh, and N.J. Buckley. 2004. Distinct RE-1 silencing transcription factor-containing complexes interact with different target genes. *J. Biol. Chem.* 279:556–561. doi:10.1074/jbc.M310353200

Bergersen, L.H., and V. Gundersen. 2009. Morphological evidence for vesicular glutamate release from astrocytes. *Neuroscience*. 158:260–265. doi:10.1016/j.neuroscience.2008.03.074

Bezzi, P., and A. Volterra. 2001. A neuron-glia signalling network in the active brain. *Curr. Opin. Neurobiol.* 11:387–394. doi:10.1016/S0959-4388(00)00223-3

Bezzi, P., M. Domercq, L. Brambilla, R. Galli, D. Schols, E. De Clercq, A. Vescovi, G. Bagetta, G. Kollias, J. Meldolesi, and A. Volterra. 2001. CXCR4-activated astrocyte glutamate release via TNFalpha: amplification by microglia triggers neurotoxicity. *Nat. Neurosci.* 4:702–710. doi:10.1038/89490

Bezzi, P., V. Gundersen, J.L. Galbete, G. Seifert, C. Steinhäuser, E. Pilati, and A. Volterra. 2004. Astrocytes contain a vesicular compartment that is competent for regulated exocytosis of glutamate. *Nat. Neurosci.* 7:613–620. doi:10.1038/nn1246

Borgonovo, B., E. Cocucci, G. Racchetti, P. Podini, A. Bachi, and J. Meldolesi. 2002. Regulated exocytosis: a novel, widely expressed system. *Nat. Cell Biol.* 4:955–962. doi:10.1038/ncb888

Bruce, A.W., I.J. Donaldson, I.C. Wood, S.A. Yerbury, M.I. Sadowski, M. Chapman, B. Göttgens, and N.J. Buckley. 2004. Genome-wide analysis of repressor element 1 silencing transcription factor/neuron-restrictive silencing factor (REST/NRSF) target genes. *Proc. Natl. Acad. Sci. USA*. 101:10458–10463. doi:10.1073/pnas.0401827101

Bruce, A.W., A. Krejcí, L. Ooi, J. Deuchars, I.C. Wood, V. Dolezal, and N.J. Buckley. 2006. The transcriptional repressor REST is a critical regulator of the neurosecretory phenotype. *J. Neurochem.* 98:1828–1840. doi:10.1111/j.1471-4159.2006.04010.x

Calegari, F., S. Coco, E. Taverna, M. Bassetti, C. Verderio, N. Corradi, M. Matteoli, and P. Rosa. 1999. A regulated secretory pathway in cultured hippocampal astrocytes. *J. Biol. Chem.* 274:22539–22547. doi:10.1074/jbc.274.32.22539

Calì, C., J. Marchaland, R. Regazzi, and P. Bezzi. 2008. SDF 1-alpha (CXCL12) triggers glutamate exocytosis from astrocytes on a millisecond time scale: imaging analysis at the single-vesicle level with TIRF microscopy. *J. Neuroimmunol.* 198:82–91. doi:10.1016/j.jneuroim.2008.04.015

Coco, S., F. Calegari, E. Pravettoni, D. Pozzi, E. Taverna, P. Rosa, M. Matteoli, and C. Verderio. 2003. Storage and release of ATP from astrocytes in culture. *J. Biol. Chem.* 278:1354–1362. doi:10.1074/jbc.M209454200

Coulson, J.M. 2005. Transcriptional regulation: cancer, neurons and the REST. *Curr. Biol.* 15:R665–R668. doi:10.1016/j.cub.2005.08.032

D'Alessandro, R., A. Klajn, L. Stucchi, P. Podini, M.L. Malosio, and J. Meldolesi. 2008. Expression of the neurosecretory process in PC12 cells is governed by REST. *J. Neurochem.* 105:1369–1383. doi:10.1111/j.1471-4159.2008.05259.x

Day, R., and S.U. Gorr. 2003. Secretory granule biogenesis and chromogranin A: master gene, on/off switch or assembly factor? *Trends Endocrinol. Metab.* 14:10–13. doi:10.1016/S1043-2760(02)00011-5

Dignam, J.D., R.M. Lebovitz, and R.G. Roeder. 1983. Accurate transcription initiation by RNA polymerase II in a soluble extract from isolated mammalian nuclei. *Nucleic Acids Res.* 11:1475–1489. doi:10.1093/nar/11.5.1475

Domercq, M., L. Brambilla, E. Pilati, J. Marchaland, A. Volterra, and P. Bezzi. 2006. P2Y1 receptor-evoked glutamate exocytosis from astrocytes: control by tumor necrosis factor-alpha and prostaglandins. *J. Biol. Chem.* 281:30684–30696. doi:10.1074/jbc.M606429200

Ekici, M., M. Hohl, F. Schuit, A. Martínez-Serrano, and G. Thiel. 2008. Transcription of genes encoding synaptic vesicle proteins in human neural stem cells: chromatin accessibility, histone methylation pattern, and the essential role of rest. *J. Biol. Chem.* 283:9257–9268. doi:10.1074/jbc.M709388200

Guardavaccaro, D., D. Frescas, N.V. Dorrello, A. Peschiaroli, A.S. Multani, T. Cardozo, A. Lasorella, A. Iavarone, S. Chang, E. Hernando, and M. Pagano. 2008. Control of chromosome stability by the beta-TrCP-REST-Mad2 axis. *Nature*. 452:365–369. doi:10.1038/nature06641

Halassa, M.M., and P.G. Haydon. 2010. Integrated brain circuits: astrocytic networks modulate neuronal activity and behavior. *Annu. Rev. Physiol.* 72:335–355. doi:10.1146/annurev-physiol-021909-135843

Hamilton, N.B., and D. Attwell. 2010. Do astrocytes really exocytose neurotransmitters? *Nat. Rev. Neurosci.* 11:227–238. doi:10.1038/nrn2803

Haydon, P.G., and G. Carmignoto. 2006. Astrocyte control of synaptic transmission and neurovascular coupling. *Physiol. Rev.* 86:1009–1031. doi:10.1152/physrev.00049.2005

Hewett, J.A. 2009. Determinants of regional and local diversity within the astroglial lineage of the normal central nervous system. *J. Neurochem.* 110:1717–1736. doi:10.1111/j.1471-4159.2009.06288.x

Hohl, M., and G. Thiel. 2005. Cell type-specific regulation of RE-1 silencing transcription factor (REST) target genes. *Eur. J. Neurosci.* 22:2216–2230. doi:10.1111/j.1460-9568.2005.04404.x

Huh, Y.H., S.H. Jeon, and S.H. Yoo. 2003. Chromogranin B-induced secretory granule biogenesis: comparison with the similar role of chromogranin A. *J. Biol. Chem.* 278:40581–40589. doi:10.1074/jbc.M304942200

Hur, Y.S., K.D. Kim, S.H. Paek, and S.H. Yoo. 2010. Evidence for the existence of secretory granule (dense-core vesicle)-based inositol 1,4,5-trisphosphate-dependent Ca2+ signaling system in astrocytes. *PLoS ONE*. 5:e11973. doi:10.1371/journal.pone.0011973

Jourdain, P., L.H. Bergersen, K. Bhaukaurally, P. Bezzi, M. Santello, M. Domercq, C. Matute, F. Tonello, V. Gundersen, and A. Volterra. 2007. Glutamate exocytosis from astrocytes controls synaptic strength. *Nat. Neurosci.* 10:331–339. doi:10.1038/nn1849

Klajn, A., C. Ferrai, L. Stucchi, I. Prada, P. Podini, T. Baba, M. Rocchi, J. Meldolesi, and R. D'Alessandro. 2009. The rest repression of the neurosecretory phenotype is negatively modulated by BHC80, a protein of the BRAF/HDAC complex. *J. Neurosci.* 29:6296–6307. doi:10.1523/JNEUROSCI.5943-08.2009

Kohyama, J., T. Sanosaka, A. Tokunaga, E. Takatsuka, K. Tsujimura, H. Okano, and K. Nakashima. 2010. BMP-induced REST regulates the establishment and maintenance of astrocytic identity. *J. Cell Biol.* 189:159–170. doi:10.1083/jcb.200908048

Kreft, M., M. Stenovec, M. Rupnik, S. Grilc, M. Krzan, M. Potokar, T. Pangrsic, P.G. Haydon, and R. Zorec. 2004. Properties of Ca$^{(2+)}$-dependent exocytosis in cultured astrocytes. *Glia*. 46:437–445. doi:10.1002/glia.20018

Malosio, M.L., T. Giordano, A. Laslop, and J. Meldolesi. 2004. Dense-core granules: a specific hallmark of the neuronal/neurosecretory cell phenotype. *J. Cell Sci.* 117:743–749. doi:10.1242/jcs.00934

Marchaland, J., C. Calì, S.M. Voglmaier, H. Li, R. Regazzi, R.H. Edwards, and P. Bezzi. 2008. Fast subplasma membrane Ca^{2+} transients control exo-endocytosis of synaptic-like microvesicles in astrocytes. *J. Neurosci.* 28:9122–9132. doi:10.1523/JNEUROSCI.0040-08.2008

Martineau, M., T. Galli, G. Baux, and J.P. Mothet. 2008. Confocal imaging and tracking of the exocytotic routes for D-serine-mediated gliotransmission. *Glia*. 56:1271–1284. doi:10.1002/glia.20696

Matyash, V., and H. Kettenmann. 2010. Heterogeneity in astrocyte morphology and physiology. *Brain Res. Rev.* 63:2–10. doi:10.1016/j.brainresrev.2009.12.001

Mortazavi, A., E.C. Leeper Thompson, S.T. Garcia, R.M. Myers, and B. Wold. 2006. Comparative genomics modeling of the NRSF/REST repressor network: from single conserved sites to genome-wide repertoire. *Genome Res.* 16:1208–1221. doi:10.1101/gr.4997306

Mothet, J.P., L. Pollegioni, G. Ouanounou, M. Martineau, P. Fossier, and G. Baux. 2005. Glutamate receptor activation triggers a calcium-dependent and SNARE protein-dependent release of the gliotransmitter D-serine. *Proc. Natl. Acad. Sci. USA*. 102:5606–5611. doi:10.1073/pnas.0408483102

Oberheim, N.A., X. Wang, S. Goldman, and M. Nedergaard. 2006. Astrocytic complexity distinguishes the human brain. *Trends Neurosci.* 29:547–553. doi:10.1016/j.tins.2006.08.004

Ooi, L., and I.C. Wood. 2007. Chromatin crosstalk in development and disease: lessons from REST. *Nat. Rev. Genet.* 8:544–554. doi:10.1038/nrg2100

Otto, S.J., S.R. McCorkle, J. Hover, C. Conaco, J.J. Han, S. Impey, G.S. Yochum, J.J. Dunn, R.H. Goodman, and G. Mandel. 2007. A new binding motif for the transcriptional repressor REST uncovers large gene networks devoted to neuronal functions. *J. Neurosci.* 27:6729–6739. doi:10.1523/JNEUROSCI.0091-07.2007

Paco, S., M.A. Margelí, V.M. Olkkonen, A. Imai, J. Blasi, R. Fischer-Colbrie, and F. Aguado. 2009. Regulation of exocytotic protein expression and Ca^{2+}-dependent peptide secretion in astrocytes. *J. Neurochem.* 110:143–156. doi:10.1111/j.1471-4159.2009.06116.x

Paco, S., E. Pozas, and F. Aguado. 2010. Secretogranin III is an astrocyte granin that is overexpressed in reactive glia. *Cereb. Cortex*. 20:1386–1397. doi:10.1093/cercor/bhp202

Paixão, S., and R. Klein. 2010. Neuron-astrocyte communication and synaptic plasticity. *Curr. Opin. Neurobiol.* 20:466–473. doi:10.1016/j.conb.2010.04.008

Palm, K., N. Belluardo, M. Metsis, and T. Timmusk. 1998. Neuronal expression of zinc finger transcription factor REST/NRSF/XBR gene. *J. Neurosci.* 18:1280–1296.

Panatier, A., D.T. Theodosis, J.P. Mothet, B. Touquet, L. Pollegioni, D.A. Poulain, and S.H. Oliet. 2006. Glia-derived D-serine controls NMDA receptor activity and synaptic memory. *Cell*. 125:775–784. doi:10.1016/j.cell.2006.02.051

Pance, A., F.J. Livesey, and A.P. Jackson. 2006. A role for the transcriptional repressor REST in maintaining the phenotype of neurosecretory-deficient

PC12 cells. *J. Neurochem.* 99:1435–1444. doi:10.1111/j.1471-4159.2006.04190.x

Pangrsic, T., M. Potokar, M. Stenovec, M. Kreft, E. Fabbretti, A. Nistri, E. Pryazhnikov, L. Khiroug, R. Giniatullin, and R. Zorec. 2007. Exocytotic release of ATP from cultured astrocytes. *J. Biol. Chem.* 282:28749–28758. doi:10.1074/jbc.M700290200

Parpura, V., and R. Zorec. 2010. Gliotransmission: Exocytotic release from astrocytes. *Brain Res. Rev.* 63:83–92. doi:10.1016/j.brainresrev.2009.11.008

Parsons, T.D., J.R. Coorssen, H. Horstmann, and W. Almers. 1995. Docked granules, the exocytic burst, and the need for ATP hydrolysis in endocrine cells. *Neuron*. 15:1085–1096. doi:10.1016/0896-6273(95)90097-7

Perea, G., M. Navarrete, and A. Araque. 2009. Tripartite synapses: astrocytes process and control synaptic information. *Trends Neurosci.* 32:421–431. doi:10.1016/j.tins.2009.05.001

Ramamoorthy, P., and M.D. Whim. 2008. Trafficking and fusion of neuropeptide Y-containing dense-core granules in astrocytes. *J. Neurosci.* 28:13815–13827. doi:10.1523/JNEUROSCI.5361-07.2008

Schoenherr, C.J., A.J. Paquette, and D.J. Anderson. 1996. Identification of potential target genes for the neuron-restrictive silencer factor. *Proc. Natl. Acad. Sci. USA*. 93:9881–9886. doi:10.1073/pnas.93.18.9881

Shimojo, M. 2008. Huntingtin regulates RE1-silencing transcription factor/neuron-restrictive silencer factor (REST/NRSF) nuclear trafficking indirectly through a complex with REST/NRSF-interacting LIM domain protein (RILP) and dynactin p150 Glued. *J. Biol. Chem.* 283:34880–34886. doi:10.1074/jbc.M804183200

Theodosis, D.T., D.A. Poulain, and S.H. Oliet. 2008. Activity-dependent structural and functional plasticity of astrocyte-neuron interactions. *Physiol. Rev.* 88:983–1008. doi:10.1152/physrev.00036.2007

Tooze, S.A. 1998. Biogenesis of secretory granules in the trans-Golgi network of neuroendocrine and endocrine cells. *Biochim. Biophys. Acta*. 1404:231–244. doi:10.1016/S0167-4889(98)00059-7

Verderio, C., S. Coco, O. Rossetto, C. Montecucco, and M. Matteoli. 1999. Internalization and proteolytic action of botulinum toxins in CNS neurons and astrocytes. *J. Neurochem.* 73:372–379. doi:10.1046/j.1471-4159.1999.0730372.x

Volterra, A., and J. Meldolesi. 2005. Astrocytes, from brain glue to communication elements: the revolution continues. *Nat. Rev. Neurosci.* 6:626–640. doi:10.1038/nrn1722

Wagoner, M.P., K.T. Gunsalus, B. Schoenike, A.L. Richardson, A. Friedl, and A. Roopra. 2010. The transcription factor REST is lost in aggressive breast cancer. *PLoS Genet.* 6:e1000979. doi:10.1371/journal.pgen.1000979

Wang, D.D., and A. Bordey. 2008. The astrocyte odyssey. *Prog. Neurobiol.* 86:342–367.

Westbrook, T.F., E.S. Martin, M.R. Schlabach, Y. Leng, A.C. Liang, B. Feng, J.J. Zhao, T.M. Roberts, G. Mandel, G.J. Hannon, et al. 2005. A genetic screen for candidate tumor suppressors identifies REST. *Cell*. 121:837–848. doi:10.1016/j.cell.2005.03.033

Westbrook, T.F., G. Hu, X.L. Ang, P. Mulligan, N.N. Pavlova, A. Liang, Y. Leng, R. Maehr, Y. Shi, J.W. Harper, and S.J. Elledge. 2008. SCFbeta-TRCP controls oncogenic transformation and neural differentiation through REST degradation. *Nature*. 452:370–374. doi:10.1038/nature06780

Wilhelm, A., W. Volknandt, D. Langer, C. Nolte, H. Kettenmann, and H. Zimmermann. 2004. Localization of SNARE proteins and secretory organelle proteins in astrocytes in vitro and in situ. *Neurosci. Res.* 48:249–257. doi:10.1016/j.neures.2003.11.002

Zenisek, D., J.A. Steyer, M.E. Feldman, and W. Almers. 2002. A membrane marker leaves synaptic vesicles in milliseconds after exocytosis in retinal bipolar cells. *Neuron*. 35:1085–1097. doi:10.1016/S0896-6273(02)00896-6

Zhang, Q., and P.G. Haydon. 2005. Roles for gliotransmission in the nervous system. *J. Neural Transm.* 112:121–125. doi:10.1007/s00702-004-0119-x